



An investigation into structural discretisation as a first-order and pilot framework to understand groundwater–stream water connectivity at a reach scale

T. Shakhane¹ · F. D. Fourie²

Received: 30 January 2018 / Accepted: 4 July 2018 / Published online: 10 July 2018
© Springer Nature Switzerland AG 2018

Abstract

This study undertook a structural discretisation as a first-order and pilot framework to understand groundwater–stream connectivity at a local to reach scale. Structural discretisation was used as the categorisation of hydrogeological landscapes, where areas having relatively uniform geology and hydrogeological characteristics were conceived of as a single-hydrologic landscape. The results of the study led to the development of reach-scale groundwater–stream typologies, a new paradigm recommended as a first-order and pilot tool to establish a groundwater–surface water interaction framework in similar settings. The typology on the southeastern side reach of the study area is the lateral contact type where groundwater enters the riparian area aquifer from the terrestrial area aquifer through the laterally continuous alluvial gravel sequence. Therefore, over-abstraction from the terrestrial and/or riparian area aquifer may result in the loss of baseflow into the river. The confined contact-type typology operates on the northern reach where the groundwater–surface exchange primarily takes place between the stream and the riparian area aquifer because, due to low-hydraulic conductivities, the terrestrial area aquifer only permits little groundwater to enter or leave the terrestrial area aquifer. In this case, progressive over-abstractions from the riparian area will primarily draw water originating from the stream through transmission losses, resulting in progressively induced stream infiltration. Consequently, groundwater–surface water interaction typologies can also play a key role in the formulation of conjunctive water resource management for greater water supply security and stability.

Keywords Structural discretisation · Hydrogeological landscapes · Structural connectivity · Terrestrial area aquifer · Riparian area aquifer · Typologies

Introduction

Groundwater and surface water are not isolated components of the hydrological system, but are generally hydraulically connected (Winter et al. 1998; Brodie et al. 2007; Kalbus 2009). Hydraulic connectivity in this study is a concept that describes inter-movement of water between hydrogeological landscapes, i.e., the riparian zone (riparian area aquifer), the upland zone (terrestrial area aquifer) and surface water

bodies. This concept is used in this study to provide a framework that enhances understanding of groundwater–surface water interaction (GSI). The GSI is an important application of understanding static (structural) and dynamic (functional) connectivity between hydrogeological landscapes and surface water bodies (Dahl et al. 2007). The exchange flow between groundwater and surface water is more dictated by aquifer properties, such as the distribution and magnitude of hydraulic conductivities of the ambient geological formation (Sophocleous 2003). Consequently, the GSI can largely be explained almost accurately with a consideration of the subsurface geology and its associated properties controlling the groundwater flow system. This means that the GSI must be investigated by a prerequisite consideration of structural connectivity to establish an acceptable pilot GSI framework. Structural connectivity is used in this work to refer to an extent to which hydrogeological landscapes and surface water bodies are physically linked to one another

✉ T. Shakhane
shakhanet@gmail.com

¹ GCS PTY. (LTD), P.O. Box 2597, Rivonia, Johannesburg, South Africa

² Institute for Groundwater Studies (IGS), University of the Free State, P.O. Box 339, Bloemfontein 9300, South Africa

and how this link could influence water transfer patterns and flowpaths.

Typically, investigations of GSI entail measurements and predictions of surface water–groundwater partition between involved water bodies. Investigation is done either through direct measurements (e.g., river bed piezometers and tracers that directly measure magnitude of water flow) or indirect measurements (e.g., groundwater level measurements and hydraulic conductivity as components of Darcy's law for quantification of exchange water flux) (Kalbus et al. 2006). For these kinds of measurements, the choice of spatial locations for measurements is critical (Palmer 1993). However, selecting locations at which measurements are to be taken is often very difficult due to pervasive heterogeneities brought about by spatial distributions of subsurface structures and relevant hydraulic properties (Sophocleous 2002). To circumvent this difficulty, discretising the structural connectivity may be considered an essential activity for GSI studies. Without such discretisation, it would be difficult to decide on the positions of the relevant measurements that would allow investigation of the properties of the different units forming part of the GSI system. Structural discretisation is used in this work as the categorisation and classification of hydrogeological landscapes that exhibit hydrogeologically unique characteristics. Hydrogeological characteristics such as the distribution and magnitude of hydraulic conductivities or transmissivities influence subsurface transfers, and therefore, connectivity between the hydrogeological landscapes (Freeze and Witherspoon 1967; Huff et al. 1982; Wolock et al. 1997; Sophocleous 2002, 2003; Uchida et al. 2005).

In the GSI characterisation, the description of hydrological landscapes needs to include a geological framework and the description of hydraulic properties of the said geological framework. Hydraulic properties of aquifers and confining layers adjacent to streams significantly impact the spatial distribution of groundwater–surface water exchanges. Geological units with different permeabilities also affect seepage distribution in surface water beds (Winter 2001). Considering these effects, an area could be subdivided into units likely to have different groundwater flow fields, where areas having relatively uniform geology and distribution and magnitude of hydraulic conductivities could be conceived of as a single hydrologic landscape unit. Therefore, the aim of the present study is to discretise the hydrogeological landscapes so as to delineate structural connectivity between groundwater and surface water bodies at a local to reach scale (0.01–5 km).

Materials and methods

The materials and methodology of the study specifically seek to:

- (a) Delineate different zones that could be indicative of the presence of different hydrogeological units forming part of the GSI system. The main question addressed by the investigation is: what are the structural controls on the hydrological connectivity between the various units? The question is addressed through geoelectrical investigations to define and delineate between different subsurface structural units, each with their own characteristic properties related to the retention and transmission of water.
- (b) Determine the distribution of individual properties of transmission of groundwater (transmissivities and hydraulic conductivities) within and between hydrogeological landscapes as discretised in (a). This objective is addressed by application of slug tests.
- (c) Subsequently, create reach-scale typologies operating along the reaches of the subject area by linking the results obtained in (a) and (b). The typologies are adapted from Dahl et al. (2007).
- (d) Characterise sources and pathways of water between hydrogeological landscapes so as to validate the GSI typologies developed in (c).

Site description

The study was undertaken at the reach to local scale (0.01–5 km) Modder River groundwater–surface water interaction (GSI) research site. The site has been established on the farm Bultfontein that is situated in the Free State province, 40 km north-west of the city of Bloemfontein, South Africa (Fig. 1). It is divided into the northwestern (NW) and the southeastern (SE) sides by the Modder River on which the Krugersdrift Dam has been built as part of the Modder River Government Water Scheme. The Modder River Government Water Scheme was developed to support downstream irrigation, including approximately 55 weirs from which local farmers abstract water for irrigation. The GSI research site was developed between the first weir and the dam wall between which the horizontal river stretch is approximately 3 km long. The weirpool stage is maintained almost constant for both winter and summer by the constant release of water from the Krugersdrift Dam sluice gates, either at regular intervals or if the weir pool level drops significantly; consequently, within the weir, the river stage is relatively higher (Shakhane et al. 2017).

The geology is predominantly made up of thick succession of Quaternary deposit, Beaufort Group (Adelaide subgroup) and Ecca group of the Karoo Sequence. The lithology of the Beaufort and Ecca Group in the study area comprises shale (from dark-bluish green to grey massive shale) and siltstone. The area is interspersed in places with Jurassic Karoo dolerites that typically intruded the Karoo Supergroup during the Jurassic Era. The quaternary deposits present on the

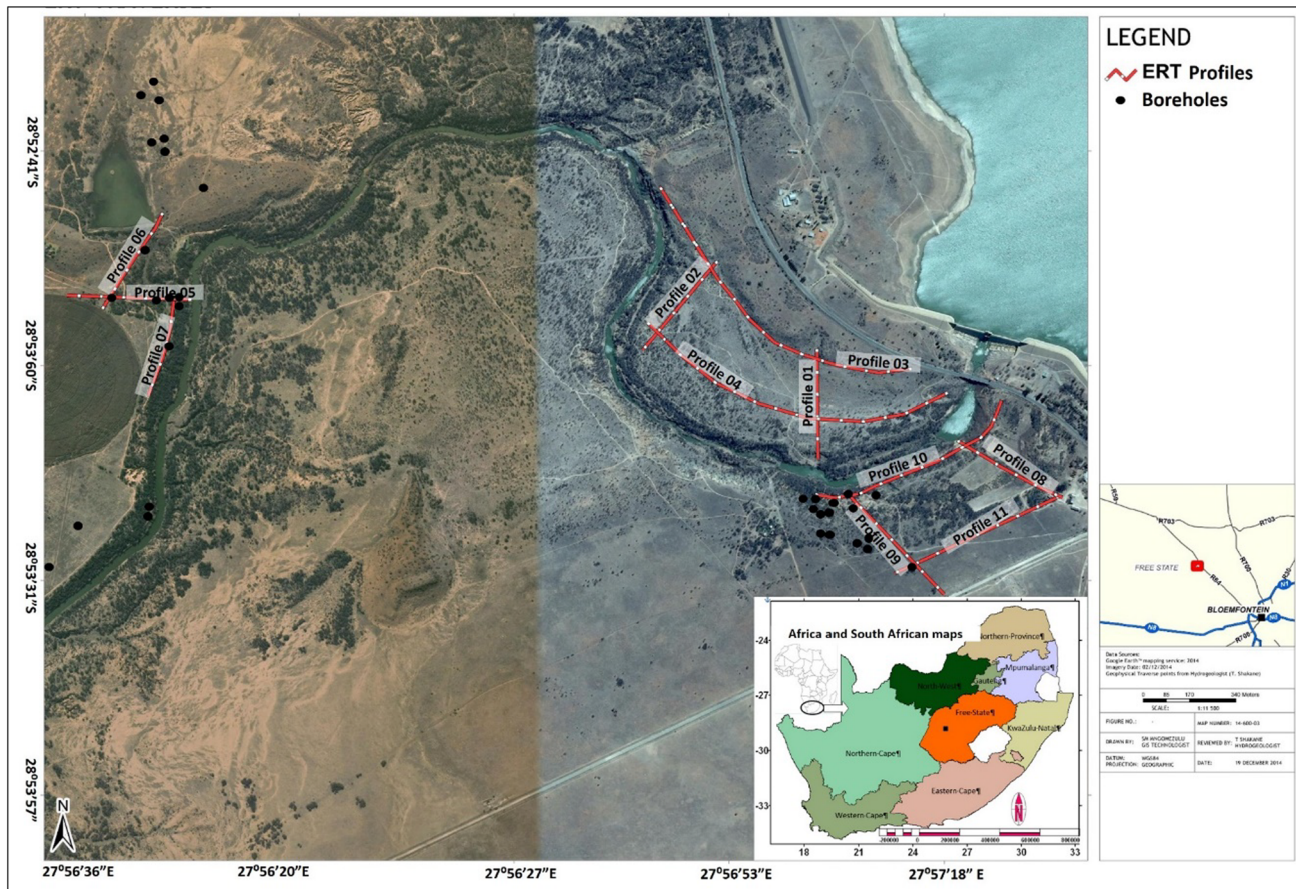


Fig. 1 Geographical setting of the study area

study site include calcrete, limestones, calcified pandunes and red to grey aeolian sands. The calcrete is mostly overlain by shallow wind-deposited sediments typical of palaeochannel; palaeochannel in the arid zone are usually covered by quaternary aeolian sand deposits in the form of sand sheets or dunefields (Magee 2009). In some other parts, the calcrete is visible on the surface and is characterised by “wormy” appearance as a result of non-uniform cementation. Typical of the quaternary deposits of the Karoo Basin, deposits of unconsolidated alluvial material occur near the stream and primarily consist clay and silt, with some continuous lenses of sand and gravel. The shale formation is the bedrock on which the unconsolidated sediments have been deposited. The average thickness of the unconsolidated overlying sediments is approximated to be about 10 m above the shale bedrock (Gomo et al. 2013).

Major characteristic of the Karoo Supergroup aquifers (which consist mainly mudstone, shale and siltstone) is their low permeability. Consequently, the majority of boreholes drilled in Karoo formations have very low yields, typically below 1 l/s; the formations may contain large quantities of water, but are not able to release it readily or economically

over small areas (Woodford and Chevallier 2002). The Ecqa Group consists mainly shales which are part of the fine-grained argillaceous rocks formed by compaction and lithification of clay and mud deposits. Due to the compaction, shales usually have very reduced porosities and are poorly sorted; consequently, they usually do not yield economical amount of groundwater. However, some scholars (e.g., Botha 1998; Woodford and Chevallier 2002) have warned against neglecting the Ecqa rocks as possible sources for groundwater, especially the deltaic sandstone facies.

The Adelaide Subgroup of the Beaufort Group on the other hand has been intruded, in some places, by dolerite sills and dykes. Groundwater in these instances occurs in joints, fractures and contact zones, weathered dolerite zones, weathered and jointed sedimentary rocks and bedding planes (Botha 1998). From a hydrogeological point of view, these properties are amongst the most important geological structures of the Adelaide Subgroup. More than 25% of the 3194 boreholes surveyed in the Karoo Supergroup are drilled into or alongside dolerite dykes with yields ranging between 0.5 and 2.0 l/s (Meyer 2003). Saturated alluvial deposits, with an estimated thickness range of 5–50 m, often form

an important component of composite bedrock aquifers, which are limited in extent to a thin strip along the main river courses and supply large volumes of groundwater to many towns in the Karoo (Woodford and Chevallier 2002). It is this saturated alluvial deposits that form primary aquifers from which the local communities depend on for water supply for agricultural and domestic use. This groundwater supplies are used conjunctively with withdrawals from weirpools, where the Krugersdrift Dam acts as a buffer for stabilizing water supply to the weirs.

Geoelectrical survey

The georesistivity technique was used to gain insight into the subsurface material properties based on the distribution of resistivities. The technique involves injection of a DC electrical current into the earth through two current electrodes inserted into the ground and the resultant electrical potential difference measured between two other electrodes (the potential electrodes). From the magnitude of the injected current and the magnitude of the measured potential difference, and by taking the distances between the various electrodes into account, an apparent resistivity for the subsurface is calculated. The apparent resistivity values recorded along a given traverse are processed to obtain a model of the resistivity distribution in the subsurface. In the present study, the geoelectrical survey was undertaken using a modern multi-electrode resistivity surveying technique known as electrical resistivity tomography (ERT). The ERT survey was conducted using the Lund Imaging System by ABEM using 4 100 m multi-core cables with 21 take-outs each. During the ERT survey, the distances between the electrodes (two out-current electrodes and two inner-potential electrodes) are varied based on a chosen four-electrode array configuration, e.g., Wenner, Schlumberger, dipole–dipole, etcetera. In all of the array configuration listed, the vertical resolution of the subsurface resistivities is achieved by increasing the distance between the electrodes while the horizontal resolution is achieved by moving the electrodes laterally across the surface. The ultimate result is a 2D collection of raw resistivity measurements (distribution) at different depths along a given survey line.

In this study, data were recorded along 11 ERT Traverses (Fig. 1), ranging in length between 400 and 2000 m, using the standard Wenner (alpha) and the standard electrode spacing of 5 m allowing for a mean average probing depth of 62 m. The standard Wenner (alpha) geometry was preferred because it is less sensitive to noise and has a high signal-to-noise ratio, therefore, it is less prone to errors emanating from poor electrode grounding and other related noise sources. The data were appropriately edited, processed and ultimately inverted using the RES2Dinv inversion algorithm by Loke and Barker (1996). The resultant 2D inversion data

were then interpreted based on a link between apparent resistivity characteristics/distributions and subsurface material properties as per the aim of the study. Prior to the inversion of the data, the following processing and editing steps were undertaken on the raw data collected:

- noisy data were checked on each profile (e.g., –ve values),
- bad data points were checked (e.g., large single data point anomalies),
- a trial for the inversion data was made and an initial model performed to check the RMS error between the observed and calculated apparent resistivity (bad data points with large RMS errors would be cut-off from the original data using the RMS error statistics bar chart in RES2D program), and,
- final inversion model with least RMS (a rule of thumb is the data points with a percentage difference below 100% on the RMS error statistics bar chart).

In situ slug tests

Numerous methods exist for characterising the distribution and magnitude of hydraulic conductivities as part of estimation and process identification in the groundwater–surface water interfaces. Kalbus et al. (2006) included slug test as one of the measurement techniques applicable in indirect determinations of water fluxes between streams and aquifers. Landon et al. (2001) practically reviewed the use of analysis methods for in situ hydraulic conductivities across the groundwater–surface water interface and concluded that slug test analysis provide reliable results at multiple measurements. Several researchers such as Nowinski et al. (2011) used the slug test for estimation of hydraulic conductivity within the point bar alluvial deposits. In this study, in situ slug tests were used, at multiple boreholes, to investigate the subsurface distribution of transmissivity and hydraulic conductivity controlling hydrologic fluxes and groundwater–surface water connections. Additionally, these tests were preferred above other methods because they allow for rapid and cost-effective determination of properties of retention and transmission of groundwater and are well suited for investigating heterogeneities (Kalbus et al. 2006). The tests were performed on 20 wells, 12 from the SE side of the study area and 8 from the NW side of the study area, by emerging a 0.009 m³ solid cylinder into the wells which instantaneously raised the water level. Subsequent head recessions were measured over time using a Solinst Levellogger programmed to an acquisition time interval of 1 s. The Levellogger was placed sufficiently deep (below the level to which the slug would sink) to avoid interference with the slug. It was connected to the Solinst Levelloader to monitor the water level progression, particularly

to determine when the water level had returned to (or almost to) the static level so that the test could be terminated. The data were analysed using the following method developed by Bouwer and Rice (1976):

$$K = \left[\frac{r_c^2}{2Lt} \right] \ln \left(\frac{R_e}{r_w} \right) \ln \left(\frac{y_0}{y} \right) \quad (1)$$

where K is the hydraulic conductivity (m/day); r_c is the inner radius of the casing (m); r_w is the well radius, or the radius of the casing plus the thickness of the gravel envelope (m); R_e is the effective radius (m) over which the drawdown, y , is dissipated; L is the length (m) of the portion of the well through which water enters (the length of the screen or perforated zone of the well); and y_0 is the drawdown (m) at time $t=0$ (Bouwer and Rice 1976). Transmissivity (T) was calculated as the product of hydraulic conductivity and saturates thickness (D) of the aquifer ($T = kD$).

Validation: isotopic analysis

Spatial variation in the stable isotopic composition of groundwater could be indicative of mixing of waters of different stable isotopic content (Payne 1990). In addition to evaluation of the lithological and structural features, Demiroğlu (2017) demonstrated the use of environmental isotope data to determine boundary conditions or physical boundaries of the groundwater systems. It is for this reason that stable environmental isotope we adopted to characterise sources and pathways of water between hydrogeological landscapes aimed at validating the GSI typologies developed in this work. This exercise was undertaken through sampling and analysis of water samples for stable isotopes of oxygen-18 and deuterium expressed as $\delta^{18}\text{O}$ and δD respectively. These isotopes are commonly used as hydrological tracers due to their properties of mass conservation (Wen 2002).

During a South African non-storm period (June–August), a total of 131 samples were collected throughout the subject area. Of the 131 samples collected, only 65 groundwater samples from observation wells and 31 water samples from the river were systematically selected, based on the structural discretisation results, for interpretation. Of the 65 groundwater samples, 40 were from the NE side, while 25 were from the NW side. The 40 samples from the NE side consisted of 26 from the riparian aquifer and 14 from the terrestrial area aquifer (TAA), while the 25 samples on the SE side included 17 from the riparian area aquifer (RAA) and 8 from the TAA. The location of the water samples relative to the sources or end-members would then indicate the relative proportion that each of the potential sources (RAA, TAA and stream) contributes to the sample (Bestland et al. 2017). Water samples were analysed using the Los Gatos Research (LGR) DT-100 Liquid Water Isotope Laser Analyser at the laboratory of the School of Bioresources Engineering and

Environmental Hydrology at the University of Kwazulu Natal (UKZN) and at the iTemba Laboratory (environmental isotope laboratory), South Africa. Each sub-sample result was reported as the average and standard deviation of injections 3–6 of the 6 sub-sample determinations. The standard deviation of the δD results was less than 1.5 permil and for the ^{18}O samples, less than 0.3 permil.

The IAEA/WMO Global Network for Isotopes in Precipitation (GNIP) established a linear correlation between δD and $\delta^{18}\text{O}$ in precipitation samples collected from a worldwide network of stations from which the Global Meteoric Water Line (GMWL) concept was established (Aggarwal et al. 2007). Differences in the amount of precipitation, temperature variations, evaporation and fractionation processes cause the relationship between the analysed stable isotopes of water δD and $\delta^{18}\text{O}$ to vary from that of the GMWL (Hoefs 2004). Therefore, the data was analysed using the GMWL graph (Craig 1961) so as to characterise sources and pathways of water across hydrogeological landscapes so as to validate the developed GSI typologies.

Results and discussion

Geoelectrical survey

In this section, the results of the geoelectrical surveys are presented as two-dimensional (2D) inversion resistivity models of the subsurface. During interpretation of these models, the observed inversion resistivity variations are associated with changes in the lithology and the degree of water saturation of the said lithological units. Specific attention is given to the interpretation of the structural connectivity between these units and the implication on the groundwater–stream water interaction. In the models, the horizontal (x)-axis represents the position along the survey line, while the vertical (z)-axis represents the depth below surface, both given in metres (m) and/or metres below ground level (mbgl). The same colour scale, presented in ohm per metre (Ωm), is used on all the survey traverses to draw comparisons between the inverse resistivity models. The inverse resistivity models are juxtaposed to borehole lithological data (where available) graphically developed by Windows Interpretations System for Hydrogeologist (WISH) and key cut-bank exposures (good or frequent enough) to aid the interpretation.

Northwestern side

Figure 2 shows the positions and orientations of ERT Traverse 01 and Traverse 02. Both these traverses were located on the inside bend of the river, and were laid out approximately perpendicular to the river. In addition, shown in Fig. 2 are the inverse resistivity models obtained from Traverse 01 and

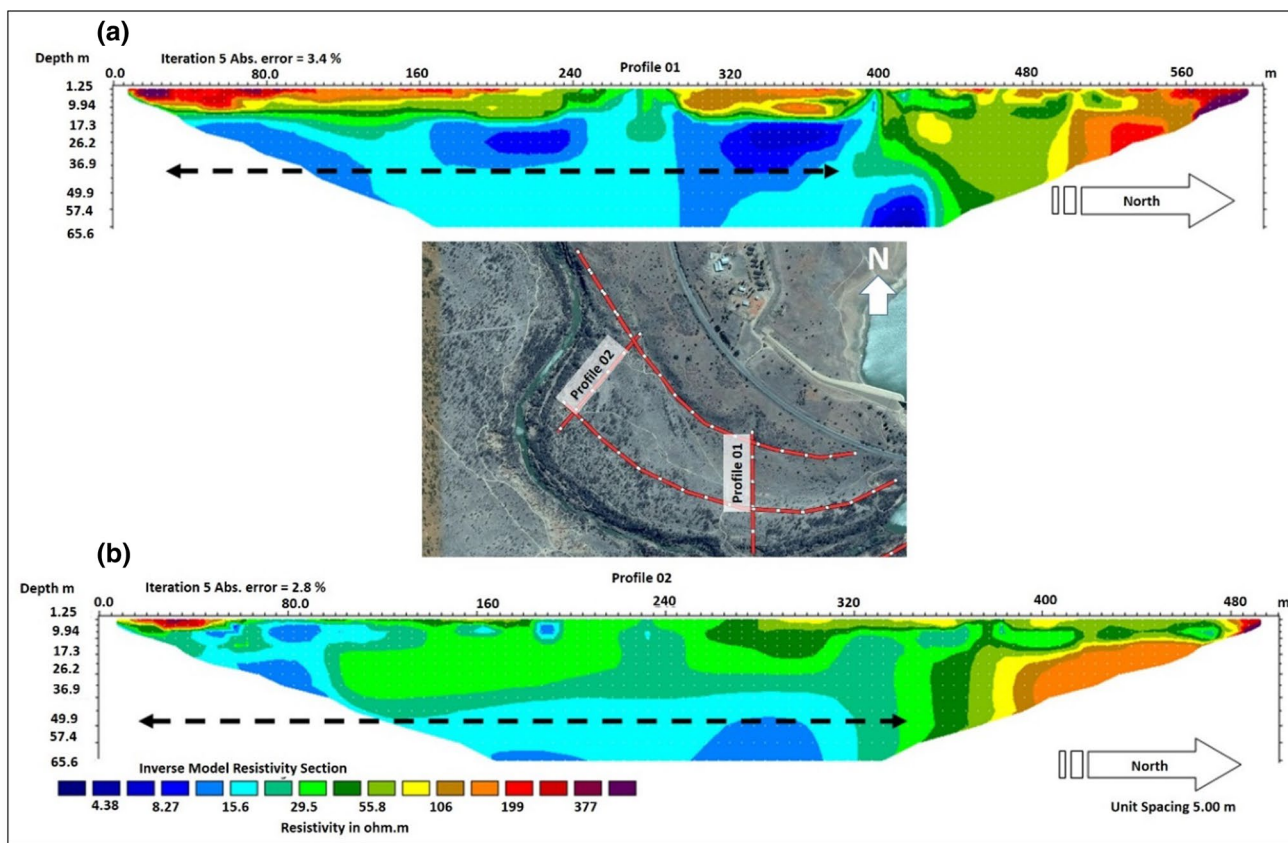


Fig. 2 Inverse resistivity models for **a** Traverse 01 and, **b** Traverse 02 (black-dotted arrows indicate the possible exchange of water between the river and the ambient aquifers)

Traverse 02. On Traverse 01, there is first the clearly defined uppermost model area, generally ranging in model resistivity from 30 to 400 Ωm. This area extends to a depth of approximately 18 mbgl below which is a more conductive area with resistivity values generally ranging from 4 to 16 Ωm. Based on the field photographs of the river cut-bank exposures (refer to Fig. 3), the top resistive area is interpreted to be a relatively dry alluvial sand deposit. This deposit overlies the coarser and more conductive (due to water saturation) area of alluvial deposit, possibly interspersed with silty clay (< 10 Ωm). The conductive layer extends farther towards the end of the resistivity inversion model before it abruptly encounters a relatively more resistive TAA from position $x \approx 400$ m to the end of the inverse model. These observations suggest that the RAA extends to a distance of ~400 m from the river. The inverse resistivity model of Traverse 02 displays almost similar resistivity distribution and characteristics; the only contrasting feature being that the RAA appears to extend to a distance of ~360 m from the river beyond which is presumably the TAA.

Both Traverse 03 and Traverse 04 were surveyed approximately parallel to the river and placed on the inside bend of the meander and across Traverse 01 and Traverse 02 (Fig. 4).



Fig. 3 A cut-bank exposure of the interbedded sand and gravel

Traverse 03 extends across the TAA which is intersected by the outside bend of the meander near position $x \approx 1\ 040$ m. At this location, the river bank exposures reveal that Traverse 03 extends across a dolerite sill (intruded into mudrock) with more resistive sub-rounded corestones surrounded by

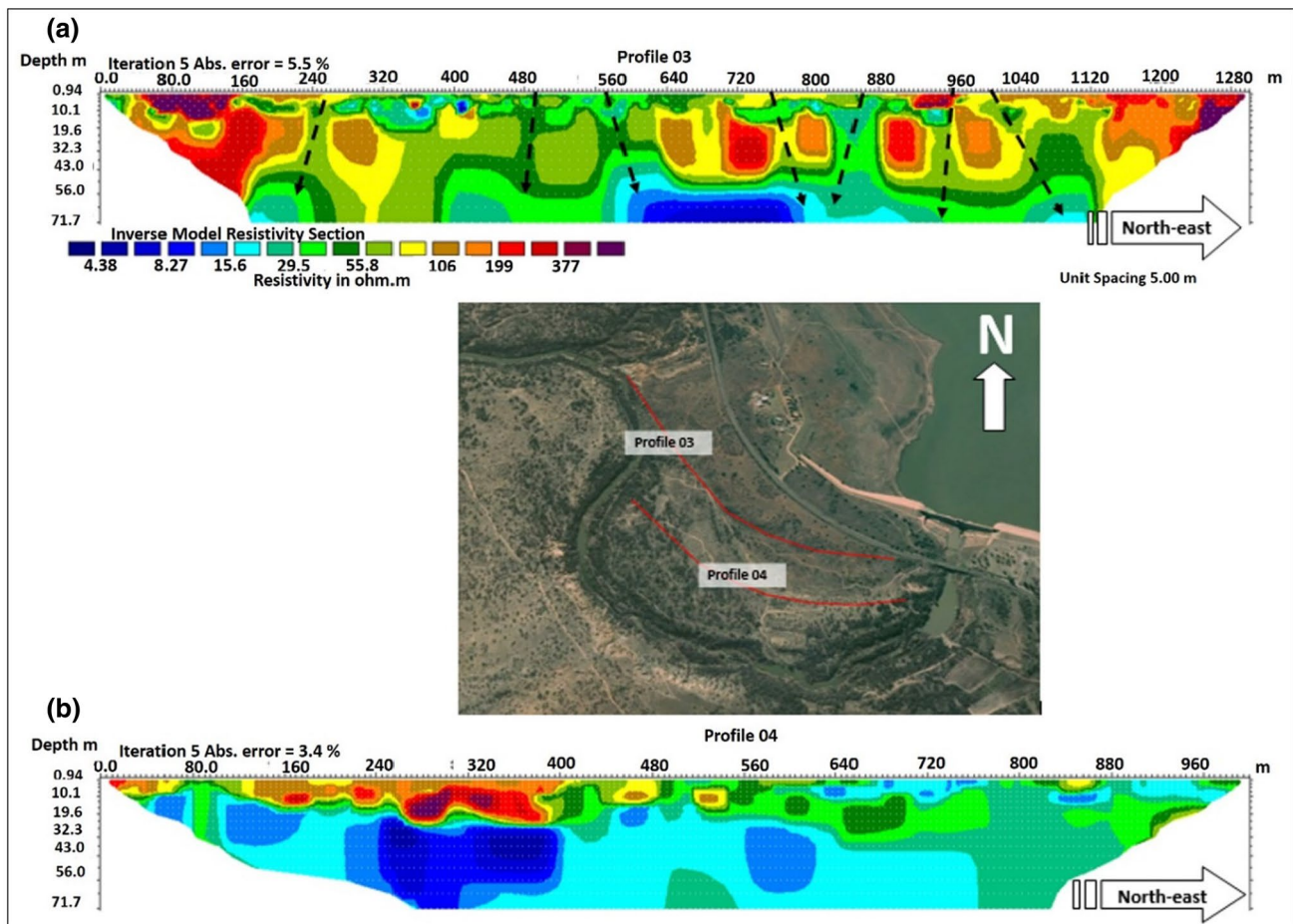


Fig. 4 Inverse resistivity models for **a** Traverse 03 and, **b** Traverse 04

porous zones of grus and rubbles (Fig. 5a). The corestones are rounded by spheroidal/onion-skin weathering and appear in the resistivity model of Traverse 03 as pockets of high resistivities (200–500 Ωm). The country rock (mudrock) exhibits splits and fracture planes which, together with the porous zone of rubble and broken rock of the dolerite rock, provide excellent avenues for the flow of water. These avenues are imaged in the resistivity model of Traverse 03 as areas of lower resistivities (16 Ωm –56 Ωm). At a depth of approximately 45 mbgl, the inverse resistivity model is characterised by a high-saturation regime, as substantiated by field observations (refer to Fig. 5b), with resistivity lows ranging between 4 and 15 Ωm . The anastomosing mudstone system of fractures most likely serves as a gateway for water fluxes between the ambient aquifer and the stream channel (Fig. 5b). On the other hand, the inverse resistivity model of Traverse 04 shows two distinct resistivity layers. The uppermost area ranges in model resistivity approximately from 30 to 400 Ωm with an average depth of $z \approx 26$ mbgl. From the start of the model to $x \approx 600$ m along the survey traverse, the upper area consists of a saturated alluvial sand diamict with

pockets of silty clay. This survey traverse is entirely situated within the RAA and the results are in perfect agreement with the results obtained along Traverses 01 and Traverse 02 in Fig. 2 across which it was surveyed.

Traverse 05 was surveyed approximately perpendicularly to the straight channel stretch of the stream (Fig. 6). The high model resistivity (60–200 Ωm) distribution in the upper part of the inverse model probably represents dry alluvial deposit, saturated and conductive (10–16 Ωm) at depth. The interpretation of alluvial deposits is only applicable from station $x \approx 145$ m to the end of the inverse resistivity model. From the start of the model to position $x \approx 145$ m, the uppermost layer is loam to clayey loam underlain by a considerably conductive layer (4–9 Ωm) of silty clay. At $z \approx 37$ mbgl, the mudstone substratum with resistivity values of ≥ 30 Ωm is encountered. This interpretation is consistent with the log of borehole CYS1BH3 that is located at $x \approx 345$ m along the survey traverse. The water level in this borehole is 10.9 mbgl (Table 1) which corresponds to the depth of resistivity lows observed on the inverse resistivity model.

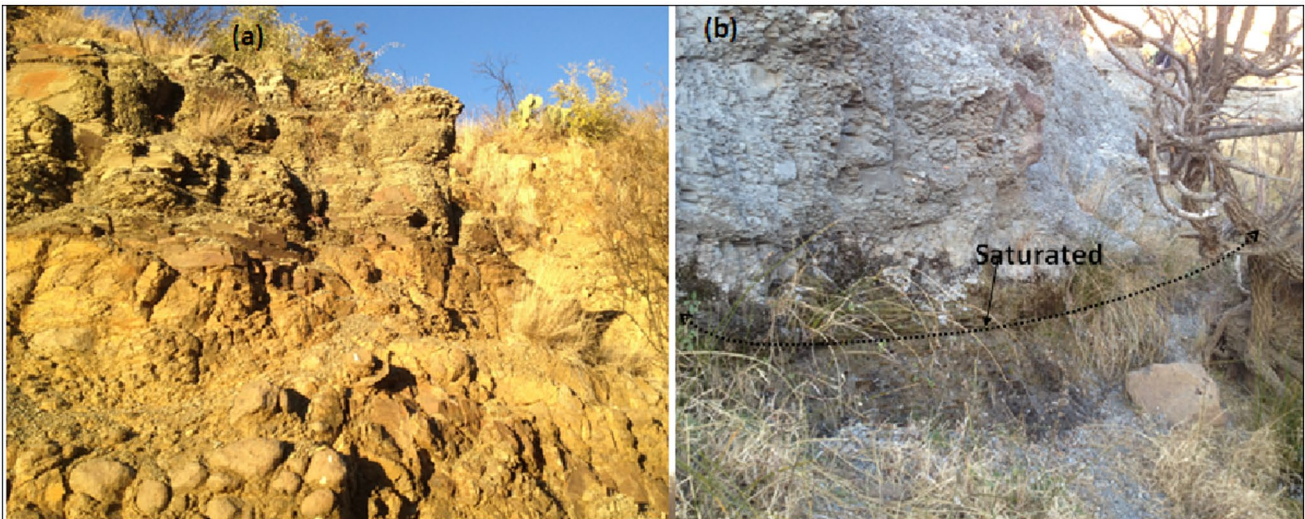


Fig. 5 The stratigraphic sequence of the river cut-bank and roadcut exposure at the field area, **a** a dolerite sill intruded into the Karoo mudrock, and **b** thick mudstone/shale saprolite underlying the dolerite sill and saturated as marked

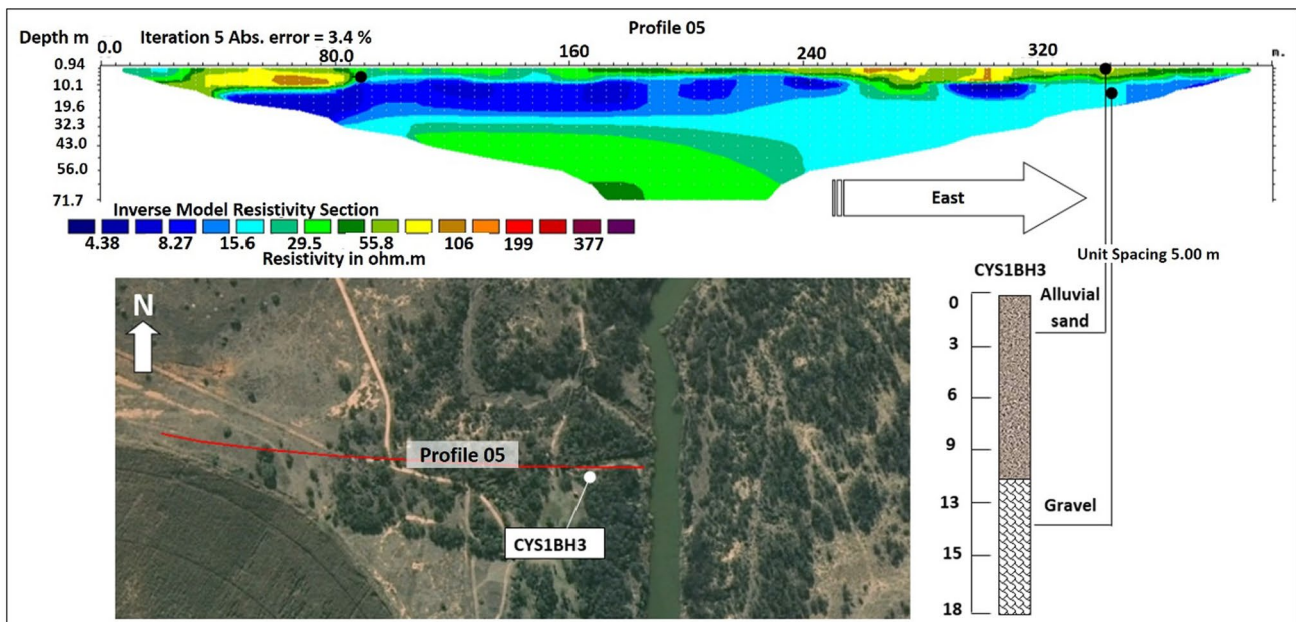


Fig. 6 Inverse resistivity model for Traverse 05

Table 1 Water level data for the boreholes located in the NW side of the study site

BH_IDs	WL (mbgl)
CYS1BH3	10.9
CYS1BH4	12.27
CYS3BH1	0.9

The water levels were measured during the resistivity survey

Both Traverses 06 and 07 were surveyed approximately parallel to the straight channel stretch of the stream (Fig. 7). Traverse 07 cuts directly across Traverse 05 and intersects borehole *CYS1BH4* at $x \approx 90$ m along the survey length. The inverse resistivity model for the resistivity distribution data collected across this traverse reveals an upper zone (~10 m deep) of relatively higher resistivity values (29–200 Ω m)

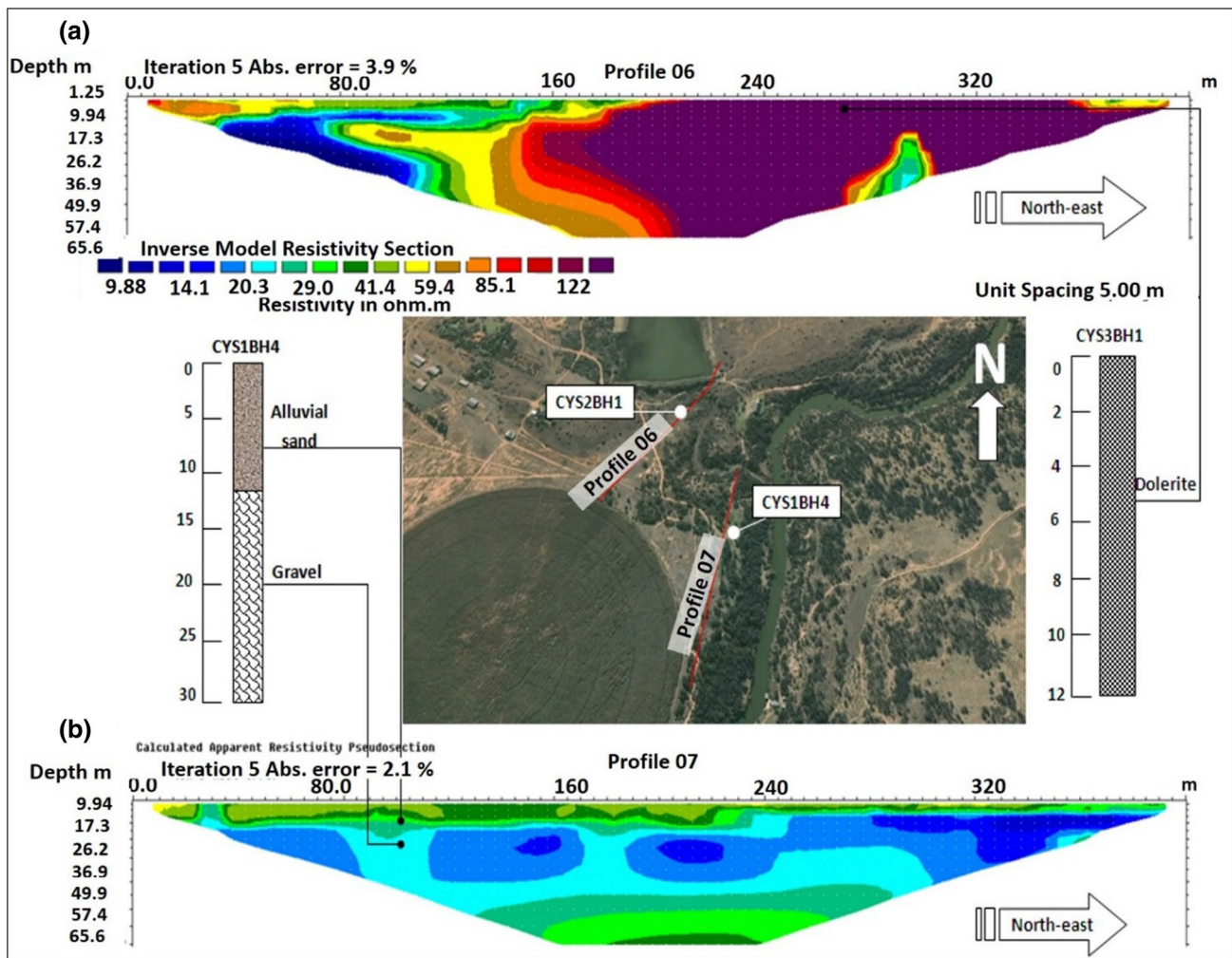


Fig. 7 Inverse resistivity model and interpretation details for **a** Traverse 06, and **b** Traverse 07

which could represent dry alluvial deposit. Below the dry alluvial deposit, the model resistivity values are generally low (9–20 Ωm) representing a saturated alluvial deposit interspersed with pockets of clay. A more resistive layer is encountered at an approximate depth of 40 mbgl which could be mudstone substratum, thereby giving an indication of the depth of the alluvial deposit unit. This interpretation is in agreement with the lithological log of borehole CYS1BH4. The log indicates that the area is characterised by alluvial sand to about 14 mbgl from where it is characterised by alluvial gravel. The water level in this borehole is 10.9 mbgl which corresponds to the depth of resistivity lows observed on the resistivity model. The resistivity model of Traverse 06 generally shows a region of lower resistivity values, approximated in the range of 5–16 Ωm , from the beginning of the model to near position $x = 120$ m, beyond which resistivities are relatively higher (≥ 59 Ωm) indicative of the location of a dolerite. This interpretation is backed up by the lithological log of borehole CYS3BH1, located near position

$x = 270$ m along the survey Traverse, and surficial exposures. Field observations confirm the presence of a dolerite (sill) outcrop with orthogonal jointing and shear fractures through which water was seen leaking (see the photograph in Fig. 8) at the of observation.

Southeastern side

The resistivity models for the data collected along Traverse 08 and Traverse 09 are shown in Fig. 9. On Traverse 08, there is first the uppermost layer ranging in model resistivity from approximately 5–17 Ωm , interpreted to be saturated alluvial deposits interspersed with silty clay. An underlying shale layer is evident with relatively higher resistivity values (30–180 Ωm). An offset towards more conductive values at 37 m depth may indicate a moist mudrock substratum. The inversion resistivity model for Traverse 09 presents an opportunity for a rather more robust interpretation that refines the interpretation of resistivity data collected



Fig. 8 A dolerite sill exposure with an abundance of orthogonal joints and shear fractures from which water was continuously leaks at the time of observation

across Traverse 8. The traverse (Traverse 09) exhibits top resistive ($< 106 \Omega\text{m}$) area beneath which lies a conductive ($5\text{--}17 \Omega\text{m}$) and saturated gravel unit interspersed with silty clay and extending to near position $x=210 \text{ m}$. The clay is revealed by field photographs of the river cut-bank exposure as the product of underlying weathering of the mudrock (Fig. 10b) under which is mudrock saprolite (Fig. 10a) with an approximate resistivity value of $30 \Omega\text{m}$. Both the gravel and saprolite may together assume the transmissive function of the connectivity between the stream and groundwater. This interpretation is supported by the lithological logs of boreholes BH1 and BH10, respectively, located near positions $x=45 \text{ m}$ and $x=305 \text{ m}$ of the resistivity model of Traverse 10 and Traverse 11. The logs indicate a shallow gravel unit in the TAA which thickens in the RAA towards the stream. This effectively implies an existence of a laterally continuous alluvial gravel sequence between the TAA and RAA. The extension of the alluvial and the saprolite to the channel cross-section serves as a gateway for water outflux from an ambient aquifer into the stream channel where the

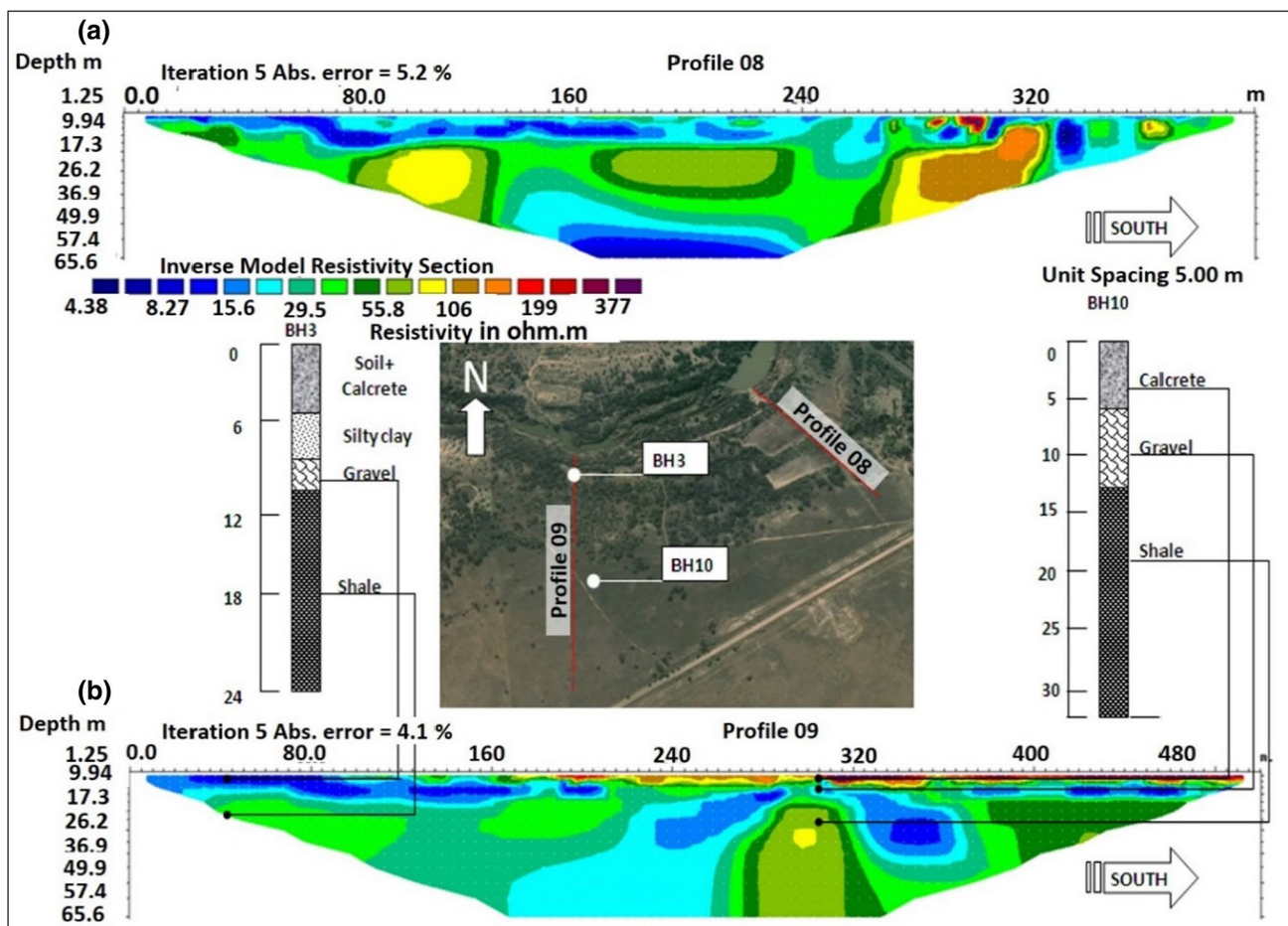


Fig. 9 Inverse resistivity model and interpretation details for **a** Traverse 08, and **b** Traverse 09



Fig. 10 River cut-bank photographs of **a** saprolite and **b** silty clay overlying the saprolite

Table 2 Water level data for the boreholes located in the SE side of the study site

BH_IDs	WL (mbgl)
BH3	2.7
BH10	9.03

The data were collected during the resistivity survey

saprolite controls ‘bulk’ or meso-scale hydraulic conductivity (Table 2).

Traverse 10 and Traverse 11 were both surveyed approximately parallel to the outside bend of the river meander (refer to Fig. 11) and perpendicular to Traverse 08 and Traverse 09. Traverse 10 is surveyed in the RAA while Traverse 11 is in the TAA. The uppermost area from the inversion models of both the traverses is interpreted to be the calcrete and alluvial sand underlain by low model resistivities (5–17 Ωm) representing saturated alluvial diamict interspersed with silty clay with an average depth of 15 m under which occurs mudrock with an approximate resistivity value of 30 Ωm . The saturated alluvial is clearly defined across profile 10 compared to the TAA (Profile 11). This interpretation is reaffirmed by a 36 m lithological log of borehole BH10 which is located at $x \approx 275$ m on Traverse 10. The log is characterised by a ~ 8 -m-thick subsurface calcrete underlain by a ~ 5 -m-thick alluvial sandy gravel deposit (Fig. 12). Alluvial deposits overlie a mudrock substratum (Fig. 12).

In situ slug tests

On the NW side of the study area, the geoelectrical survey was undertaken on two primary channel genetics, namely the inside bend of the meander and straight channel stretch

of the stream. The results reflected characteristics typical of meandering channel depositions where the inside bend of the stream is possibly reflective of lateral point-bar accretion. Since stream meandering results from bank erosion on the outside bank of the loop and deposition on the inside bank, much of the material eroded from the outside bank of a meander is deposited on the inside bank. Progressive erosion of the cut bank and accretion of the opposite point bar causes the channel to migrate creating a floodplain of deposits capped with alluvial sediment (Wolman and Leopold 1957, Ritter et al. 1973). Contrarily, a thin strip of alluvial deposition was characterised along the straight channel stretch, a feature characteristic of sediments transported and deposited by the recent flow regime (overbank deposition of sediment during floods). Nanson and Croke (1992) refer to this floodplain genetic as overbank vertical-accretion; a sandy floodplain that can be destroyed by large flood events and reconstructed by overbank deposition. The interpretation of the geoelectrical results further illustrated that the alluvial deposits are generally proximal to the stream (< 500 m) and bounded by the Ecca Group mudrock (country rock).

On the SE side of the study area, the geoelectrical survey was undertaken on the outside bend of the meander. Supported by borehole geological drill logs, the geoelectrical results indicated that the SE side is primarily characterised by an extensive and ≤ 10 m thick alluvial sediments, possibly connoting palaeochannel deposits, interspersed with palaeochannel calcrete and overlying the Ecca Group mudrock (bedrock). Deposited from laterally migrating shallow groundwater, calcrete form as replacements of a variety of sedimentary and regolith materials. This is typical of the palaeochannel in the arid settings where calcrete tends to form as replacements of a variety of sedimentary and regolith

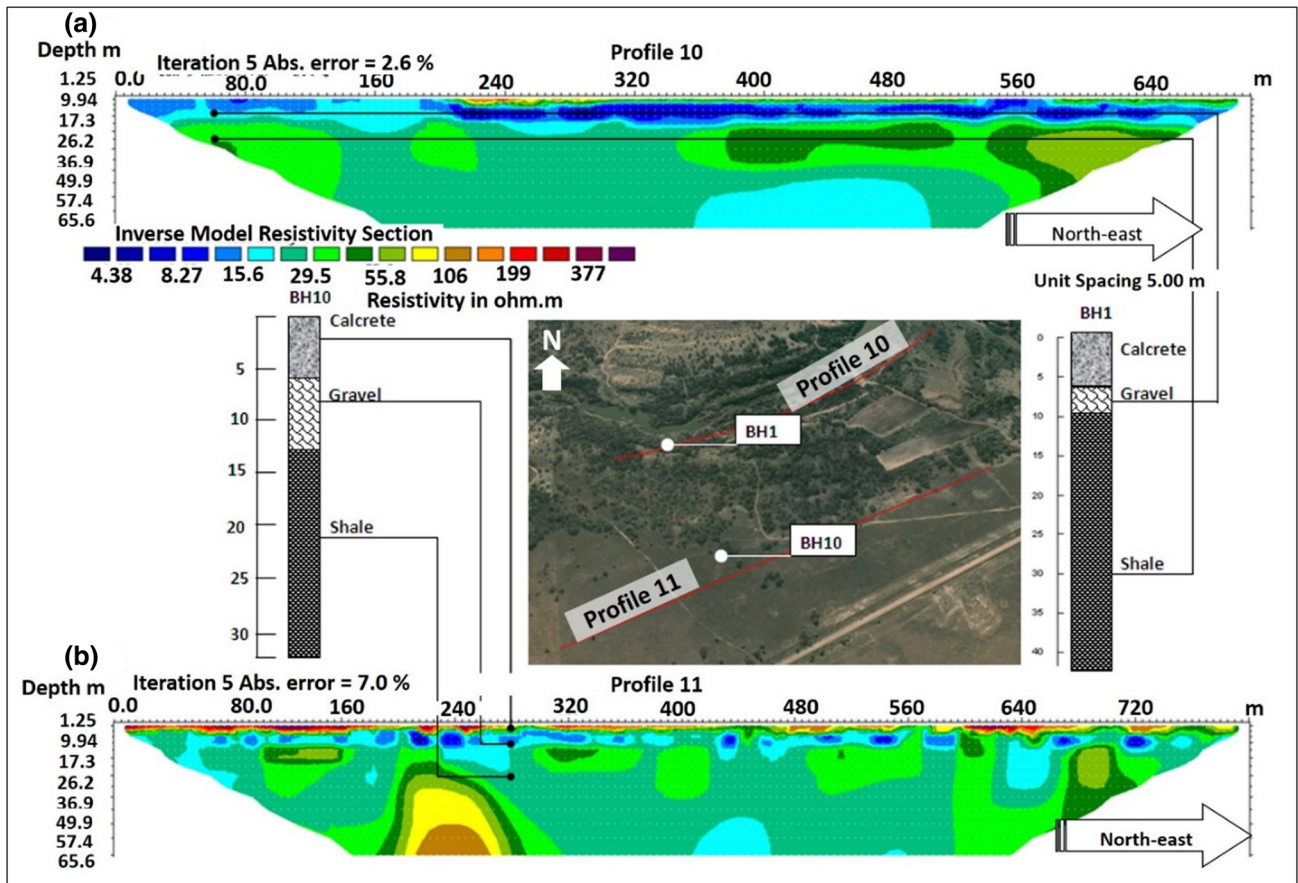


Fig. 11 Inverse resistivity models for a Traverse 10 and b Traverse 11 correlated to geological logs from boreholes BH1 and BH10

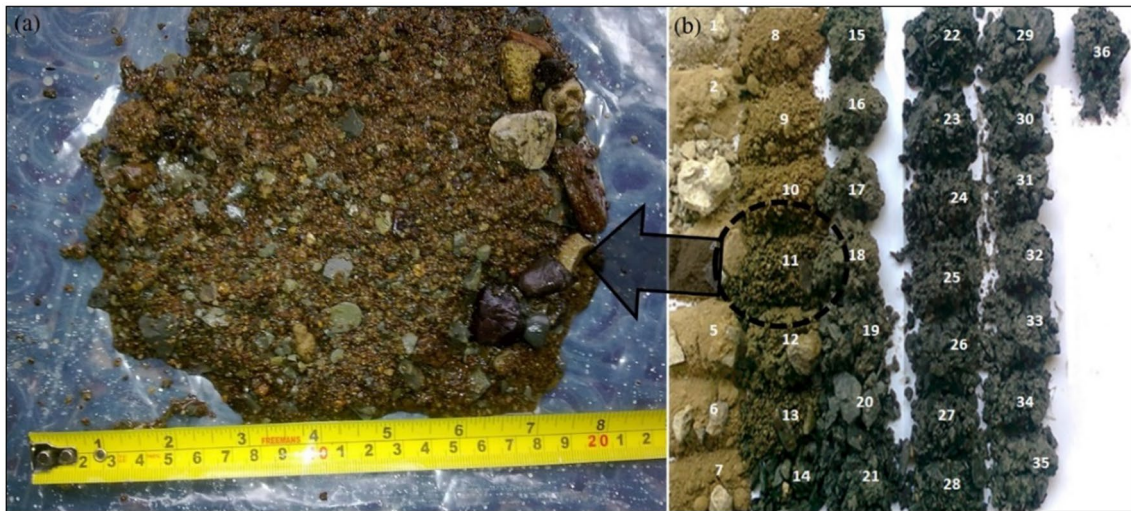


Fig. 12 Lithological log showing, a alluvial sample obtained from 11 mbgl, and b well cuttings obtained during BH10 drilling

materials. The palaeochannel deposits are active elements of the landscape and represent dynamic groundwater systems (Magee 2009). Consequently, the geoelectrical results have enabled the delineation of different zones that could be indicative of the presence of different hydrogeological units forming part of the GSI system, namely the riparian areas aquifer (RAA) and terrestrial area aquifer (TAA).

On the southeastern side, both the RAA and the TAA are stratigraphically described by a four-layer model with predominantly alluvial sand/calcrete followed by sandy alluvial gravel, saprolite and the mudstone substratum. On the northwestern side, the RAA is stratigraphically described by a three-layer model with alluvial sand layer followed by a sandy alluvial gravel unit and the mudstone substratum while the TAA is described by a two-layer model comprising silty clay and the mudstone substratum. In this regard, it can be expected that variations in clay content will result in permeability contrasts where higher clay contents correlate with lower permeability (Tables 3, 4) and could restrict the flow exchange. On the southeastern side, the range of hydraulic conductivity (K) values is 0.02–0.2 and 0.10–0.61 m/day for the RAA and TAA, respectively (Table 3). On the northwestern side, the range of hydraulic conductivity values is 0.10–0.83 and 0.002–0.1 m/day for the RAA and TAA, respectively (Table 4). From these results, the southeastern side exhibits almost uniform and high K -values, across both the RAA and TAA. In contrast, the northwestern site displays higher K -values in the riparian area aquifer, with the terrestrial aquifer characterised by much lower K -values.

GSI typology of the study area

The GSI typology on the southeastern (SE) site has been identified as the lateral regional type where the RAA is in full contact with the TAA through alluvial gravel sediments

Table 3 Estimated hydrogeological parameters of boreholes on the southeastern side

Borehole ID	K (m/day)	T (m ² /day)	Aquifer
BH1	0.02	0.1	Riparian
BH2	0.004	0.05	
BH3	0.08	0.63	
BH5	0.20	1.59	
BH6	0.2	1.33	
BH8	0.02	0.12	
BH9	0.11	0.87	
BH10	0.34	1.68	Terrestrial
BH11	0.19	0.93	
BH13	0.10	0.48	
BH12	0.23	1.17	
BH15	0.61	3.03	

Table 4 Estimated hydrogeological parameters of boreholes on the northwestern side

Borehole ID	K (m/day)	T (m ² /day)	Aquifer
CYS1BH3	0.18	0.01	Riparian
CYS1BH4	0.10	0.01	
CYS1BH5	0.20	0.09	
CYS2BH2	0.83	1.67	
CYS2BH7	0.004	0.02	Terrestrial
CYS2BH8	0.10	2.42	
CYS2BH9	0.002	0.02	
CYS4BH1	0.009	0.12	

(Fig. 13). This could facilitate a considerable degree of connectivity within these aquifers as well as between them and the river. The saprolite and the alluvial gravel unit in this case can serve as the conduits through which the TAA, RAA and the river are hydraulically in active connection. This typology assumes a mudrock substratum as a no flow or impermeable boundary such that there is no groundwater flow in the deeper permeable mudstone bedrock. In this case, the groundwater enters the RAA at the hillslope, primarily through the laterally continuous alluvial gravel sequence (characterised by well-rounded cobbles) sandwiched between the mudstone substratum and overtop

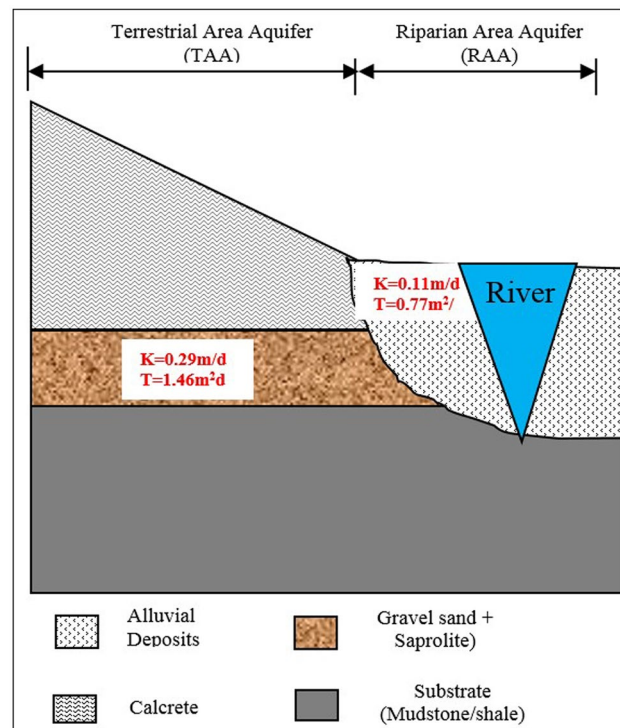


Fig. 13 Riparian hydrogeological type (lateral local) for the southeastern side of the study area (Artwork by Microsoft Word)

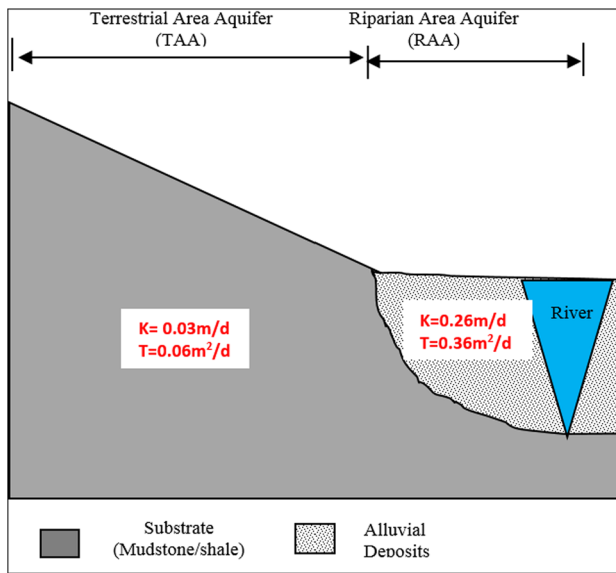


Fig. 14 Riparian hydrogeological type for the northwestern side of the study area (Artwork by Microsoft Word)

calcareous and alluvial sand (with some silt and sandy clay) semi-confining overburden.

On the northwestern site, the GSI typology has been identified as the confined contact type (Fig. 14). Based on the slug test results from wells drilled in both aquifers, the site shows a high degree of heterogeneity between the riparian and the terrestrial aquifers in terms of their hydraulic properties. Low-hydraulic conductivities have been calculated on the TAA in which case the aquifer can only permit little groundwater to enter or leave the terrestrial area aquifer. This would effectively be inimical to the groundwater water exchange between the RAA and the low-permeable TAA. In the RAA, sand and gravel are the predominant deposits with relatively much higher hydraulic conductivities which could lead to active exchanges of water between the RAA and the river. In other words, the groundwater–surface exchange actively happens between the river and the RAA (alluvial gravel, silt and sand). In fact, the groundwater flow within the RAA may be parallel to the stream channel as underflow. As simplified above, the alluvial gravel deposits form unconfined aquifers exposed at the ground surface or shallowly buried by unconsolidated permeable surficial sediment; consequently, they are prone to direct recharge from rainfall. Groundwater discharge from these aquifer is likely to involve three main mechanisms: transpiration by plants where roots can access the water table (Shakhane et al. 2017), lateral leakages and groundwater abstraction. Lateral leakages would occur according to the nature of the hydraulic connectivity between the aquifer and bounding

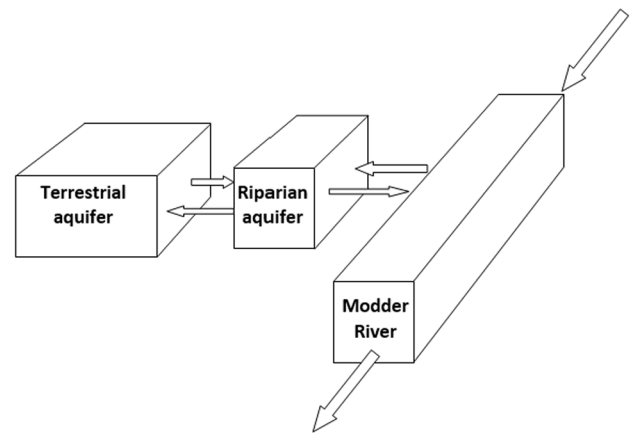


Fig. 15 A sampling programme using the concept of a three flowpath conceptual box model (Artwork by Microsoft Word)

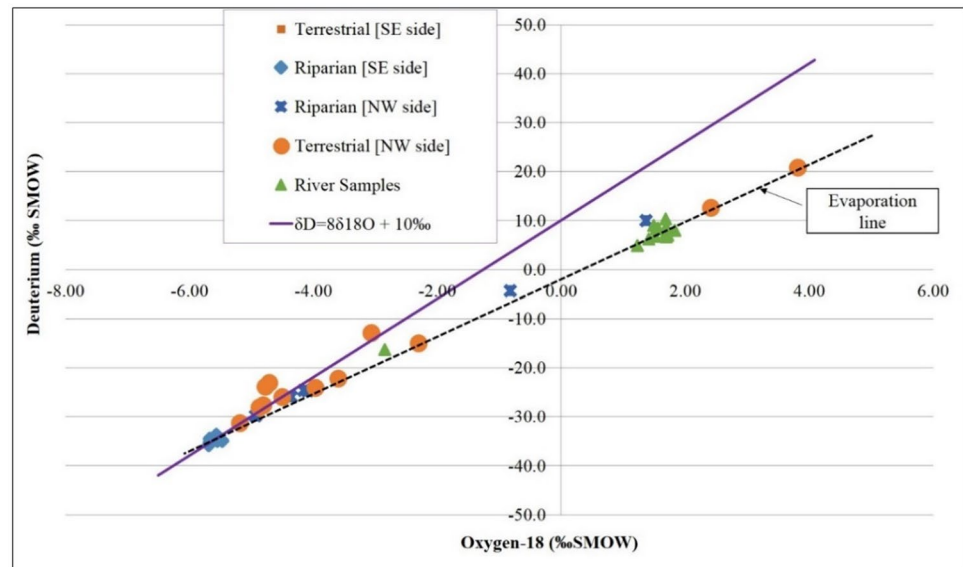
(mudrock) units, and the degree of saturation of those units relative to the palaeochannel aquifer.

Validation: isotopic analysis

Based on the information from the geophysical data and the developed GSI typologies, the conceptualisation of structural connectivity (GSI typologies) can be extended to the spatial sources of water through a three flowpath conceptual box model (Fig. 15) representing the terrestrial–riparian channel interaction continuum. The three flowpath conceptual box model is regarded as a distinctive feature in which the interaction continuum is partitioned into linked boxes representing distinct hydrogeological elements (i.e., TAA, RAA and stream channel) as conceptualised in the GSI typology development. Each of the hydrogeological elements represents the space containing water with unique chemical solutes, while the bigger arrows represent the possible transfer or flux of material into and out of the elements. As such, the movement of water between the elements could provide a pathway for exchange of chemical constituents. Since rates of water movement and geochemical interactions differ substantially between different types of hydrological landscape elements, each of the boxes may have a unique suite of dissolved ‘chemical identifiers’, such as stable isotope of $\delta^{18}\text{O}$ and δD , which can be traced back to their source areas and, therefore, be used to delineate the flowpaths. The variations in isotope composition for the RAA and TAA for both the NW and SE sides are presented in Table 5. In general, the river water ranges of isotope composition are closer to those of the NW side’s RAA than they are to the terrestrial aquifer which suggests that the GSI occurs in the river–riparian–terrestrial flowpath. On the SE side, the GSI occurs in the terrestrial–riparian–river flowpath due to the fact that

Table 5 Ranges of isotopic compositions of both groundwater and river samples

Side ID	TAA		RAA		River	
	$\delta^{18}\text{O}$	δD	$\delta^{18}\text{O}$	δD	$\delta^{18}\text{O}$	δD
NW	-5.18 to 3.82	-31.3 to 20.8	-4.94 to 1.37	-29.8 to 10.0	-2.85 to 1.83	-16.3 to 10.4
SE	-6.50 to -5.55	-35.3 to -33.8	-5.69 to -5.47	-35.8 to -34.4		

Fig. 16 Plot of $\delta^{18}\text{O}$ vs. δD for the water samples from the aquifer systems and the river

the isotope concentrations are much different from those of the river. This can be substantiated and refined clearly by the conventional $\delta^{18}\text{O}$ vs. δD GMWL diagram.

The $\delta^{18}\text{O}$ values vs. δD results for both the NW and SE sides are plotted on the conventional $\delta^{18}\text{O}$ vs. δD diagram as shown in Fig. 16. The samples from the SE are more depleted (most negative) $\delta^2\text{H}$ and $\delta^{18}\text{O}$ isotopic values which plot along the GMWL, reflecting recharge originating from the regional groundwater source. Although this characteristic isotopic signature in the data could also connote water originating from the rainfall, the sampling programme for this study was undertaken in the dry season. The GSI typology on the southeastern (SE) site has been identified as the lateral regional type where the RAA is in full contact with the TAA system through alluvial gravelly sediments which is validated by homogeneous isotopic composition across the two hydrogeological landscapes. On the other hand, the groundwater compositions from both the TAA and RAA were very different to those of the river water, indicating that the source of the groundwater in this area is by no means from the river water.

Groundwater from the RAA of the NW side of the study area is isotopically enriched (least negative) $\delta^2\text{H}$ and $\delta^{18}\text{O}$ values, while some samples are relatively more depleted (most negative). Scattered signature of stable isotope values in many occasions imply variation in the recharge mode and

transient conditions of the system in question (Madioune et al. 2014). Therefore, the observed isotopic characteristic signatures in the NW side RAA effectively reflect variable mixing of river water with recharge from the TAA system giving rise to what is referred to, in this paper, as convergent flow. In simple terms, convergence flow occurs when flow of river water and that from the TAA both flow towards and mix in the RAA. This implies that water discharging into the stream can either be groundwater, or re-emerging surface water, or a mixture of both. The river water flows into the RAA due to induced recharge associated with higher river stage relative to ambient groundwater. This characteristic occurs when the pressure heads are balanced by equal elevations of channel stage and groundwater head as observed on the subject area (Fig. 17). The river stage could either effectively flatten the gradient between the aquifer and stream or be so large as to reverse the gradient, which would cause the stream to constantly lose water to the alluvial aquifer. Contrarily, on the SE side of the study site, groundwater seepage visibly occurs on the channel banks above the level of the channel all year round (Fig. 18). As per the typology established for the SE, the groundwater flows across the gravelly alluvial unit across the TAA into the RAA and eventually visibly seeps into the river.

The established typologies, validated by the isotopic fingerprinting, suggested that the influent and effluent

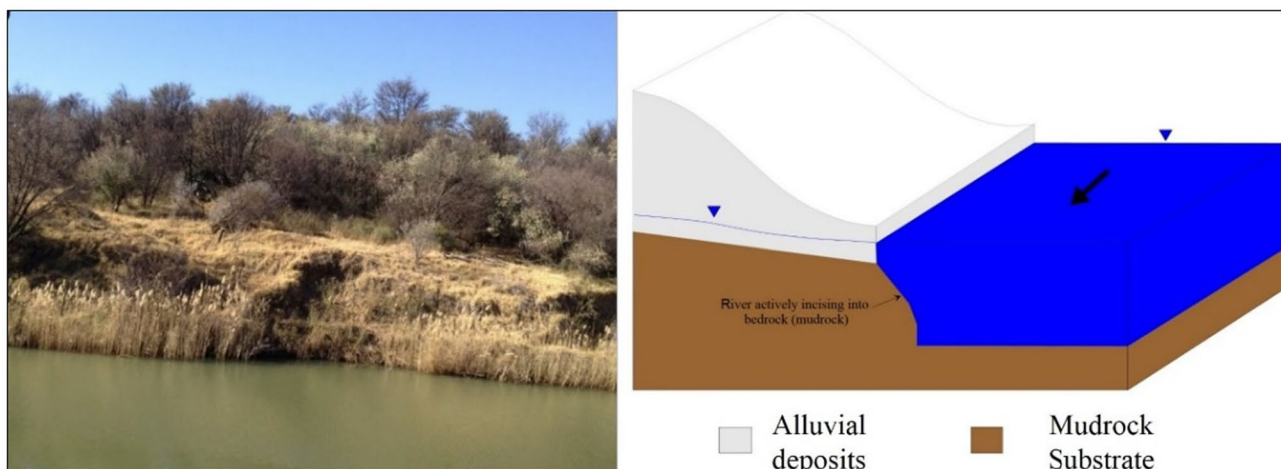


Fig. 17 Field photograph taken in winter (dry season) and a corresponding schematic illustration of channel morphology and hydrology for the NW reach of the study site (Artwork by Surfer Golden Software)

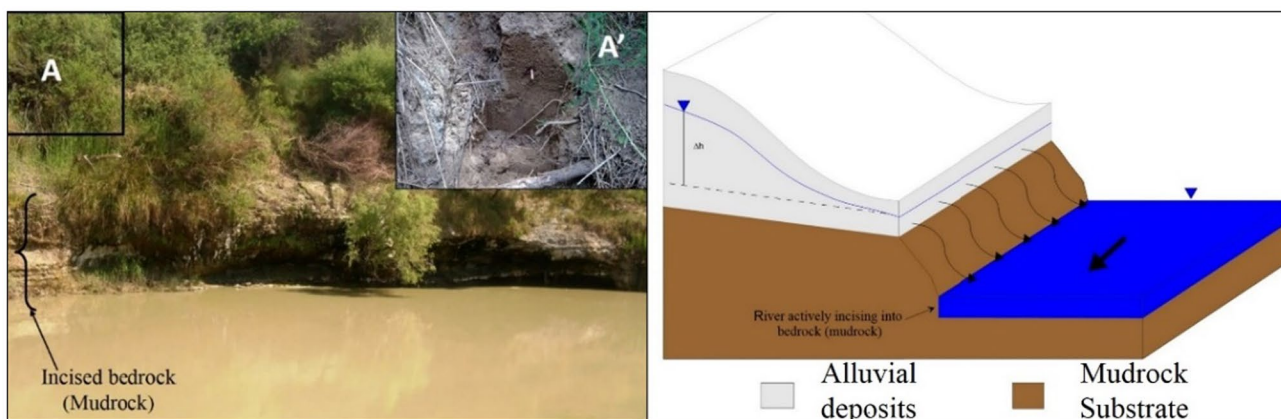


Fig. 18 Field photograph taken in summer (rainy season) and a corresponding schematic illustration of channel morphology and hydrology for the SE reach of the study site (Artwork by Surfer Golden Software)

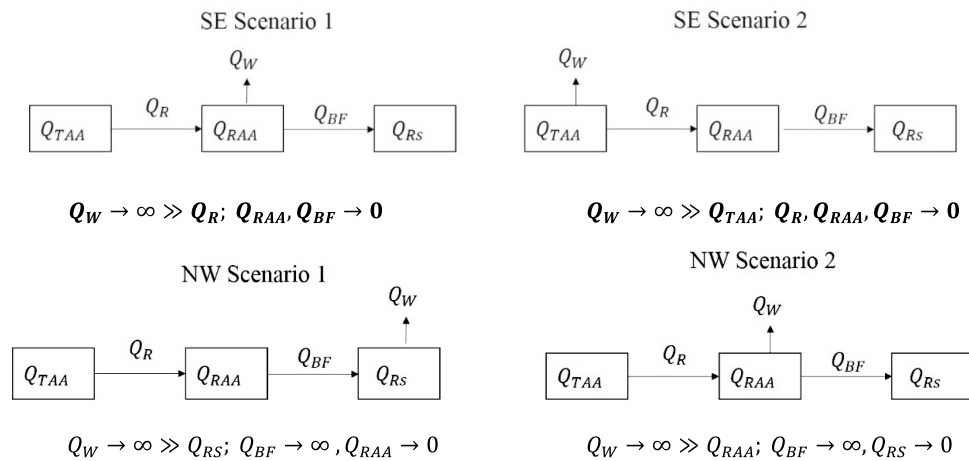
conditions occur simultaneously in the study site. The typologies have also provided the basis on which the environmental consequences of human-imposed stresses on GW systems can be assessed considering the conjunctive use of surface and groundwaters across the subject area perimeters. Based on the established typologies, there are two major scenarios of consequences resulting from increasing exploitation of GW supplies for each of the reaches (SE and NW), namely:

1. *SE Scenario 1* Where over-abstraction (Q_W) progressively exceeds the natural rate of replenishment (Q_R) of the RAA for the SE reach,
2. *SE Scenario 2* Where over-abstraction (Q_W) progressively exceeds the natural rate of replenishment (Q_R) of the TAA for the SE reach,
3. *NW Scenario 1* Where weirpool withdrawals (Q_W) are so high that the river stage is lowered far below the ambient groundwater level for the NW reach, and
4. *NW Scenario 2* Where over-abstraction (Q_W) progressively exceeds the natural rate of replenishment (Q_R) of the RAA for the NW reach.

It has been ascertained from the preceding results and interpretations that the Modder River at the research site is sustained by the regional groundwater from the (SE) reach. The laterally continuous alluvial gravel sequence is an important productive aquifer that supports the economically important agricultural and consumptive (domestic) activities of the SE inhabitants. Therefore, the most direct impacts of prolonged groundwater depletion (over-pumping) on integrated water supply will be a loss of baseflow into the

river (as illustrated by *SE Scenario 1*) and the depletion of groundwater in the RAA (as illustrated by *SE Scenario 2*). On the other hand, over-abstraction from boreholes sited in the RAA of the NW reach will effectively draw water originating from the stream through transmission losses, leading to induced infiltration or recharge causing streamflow depletion. It should be noted that this effect will not occur in the event of *SE Scenario 1 and/or SE Scenario 2* because the river in the SE reach is incised into mudrock substratum which has caused the river stage to always be far below the gravel sequence and the mudrock saprolite. Because baseflow in streams and surface vegetation are dependent on groundwater levels, change in those levels (due to *SE scenario 1 and NW Scenario 2*) can induce ripple effects on many uses and environmental values of uses that depend on groundwater and surface water.

continuous alluvial gravel sequence. The laterally continuous alluvial gravel sequence is an important productive aquifer whose over-withdrawal (over-pumping) will result in the loss of baseflow into the river. On the other hand, over-abstraction in the riparian area of the NW reach will effectively draw water originating from the stream through transmission losses resulting in progressively induced stream infiltration. The typologies have further highlighted that both the RAA and the TAA influences the GSI based on their individual subsurface material properties of groundwater storage and transmission; therefore, the outcome of this study has first highlighted that the groundwater–surface water interaction typologies are pivotal in providing a first-order framework for GSI assessment and even formulation of preliminary conjunctive groundwater and surface water resource management. Second, the study has additionally



Conclusions

The aim of the present study was to discretise the hydrogeological landscapes to delineate structural connectivity between groundwater and surface water bodies at a local to reach scale (0.01–5 km). The approach in meeting this aim provided credible process enhancing further understanding of GSI. The approach has enabled the development of reach-scale GSI typologies as a new paradigm to better understand the groundwater and surface water connectivity. The paradigm is recommended as a first step, preceding further detailed investigations, to establish a preliminary GSI framework in settings similar to the subject area. This framework will ensure that each of the hydrogeological landscapes are each adequately represented during the development of field designs of data collection programmes.

The established typologies have indicated that the Modder River at the subject area is sustained by the regional groundwater from the (SE) reaches through the laterally

highlighted key responses controlled by aquifer development, reiterating conjunctive groundwater and surface water resource management. Conjunctive water management in this study is redefined as involving the combined use of groundwater, as contained in each of district hydrogeological landscapes (riparian area aquifer, terrestrial area aquifer), to achieve public policy and management goals enabling greater water supply security and stability.

Acknowledgements This study has been undertaken as part of the the South African Water Research Commission (WRC) project titled *groundwater–surface water interactions: from theory to practice (K5/254/1)*. Therefore, the financing of the project by WRC is gratefully acknowledged. The authors also wish to acknowledge Mr. Tlali Shakhane for his help during both the geophysical survey and the entire sampling program. We wish to thank also Prof. Simon Lorentz and Mr. Cubus Pretorius who undertook most of the isotope analysis for this research. We greatly appreciate and value the recommendations and criticism of the reviewers (Dr. RC Jain and anonymous) and really acknowledge they served to make the manuscript better.

References

- Aggarwal PK, Froehlich K, Kulkarni KM (2007) Environmental isotopes in groundwater studies. In: Silveira L, Usunoff EJ (eds) *Groundwater—encyclopedia of live support systems*. EOLSS Publishers/UNESCO, Paris, pp 69–92
- Bestland E, George A, Green G, Olifent V, Mackay D, Whalen M (2017) Groundwater dependent pools in seasonal and permanent streams in the Clare Valley of South Australia. *J Hydrol Reg Stud* 9:216–235
- Botha JF (1998) Karoo aquifers, their geology, geometry and physical properties. WRC report no; 487/1/98. Water Research Commission, Pretoria
- Bouwer H, Rice RC (1976) A slug test for determining hydraulic conductivity of unconfined aquifers with completely or partially penetrating wells. *Water Resour Res* 12:423–428
- Brodie R, Sundaram B, Tottenham R, Hostetler S, Ransley T (2007) An overview of tools for assessing groundwater-surface water connectivity. Bureau of Rural Sciences, Canberra
- Craig H (1961) Isotopic variations in meteoric waters. *Science* 133:1702–1703
- Dahl MB, Nilsson B, Langhoff JH, Refsgaard JC (2007) Review of classification systems and new multi-scale typology of groundwater–surface water interaction. *J Hydrol* 344:1–16
- Demiroğlu M (2017) Identifying the groundwater basin boundaries using environmental isotopes: a case study. *Appl Water Sci* 7:1161–1167
- Freeze RA, Witherspoon PA (1967) Theoretical analysis of regional groundwater flow, II: effect of water table configuration and subsurface permeability variations. *Water Resour Res* 3:623–634
- Gomo M, van Tonder GJ, Steyl G (2013) Investigation of the hydro-geochemical processes in an alluvial channel aquifer located in a typical Karoo Basin of Southern Africa. *Environ Earth Sci* 70:227–238
- Hoefs J (2004) *Stable isotope geochemistry*. Springer, Germany
- Huff DD, Oneill RV, Emanuel WR, Elwood JW, Newbold JD (1982) Flow variability and hillslope hydrology. *Earth Surf Proc Land* 7:91–94
- Kalbus E (2009) *Spotlight on heterogeneity: measuring and modelling stream–aquifer interactions*. Thesis, University of Neuchâtel
- Kalbus E, Reinstorf F, Schirmer M (2006) Measuring methods for groundwater–surface water interactions: a review. *Hydrol Earth Syst Sci* 10:873–887
- Landon MK, Rus DL, Harvey FE (2001) Comparison of in-stream methods for measuring hydraulic conductivity in sandy streambeds. *Groundwater* 39:870–885
- Loke MH, Barker RD (1996) Rapid least-squares inversion of apparent resistivity pseudosections by a quasi-Newton method. *Geophys Prospect* 44:131–152
- Madioune DH, Faye S, Orban P, Brouyere S, Dassargues A, Mudry J, Stumpp C, Maloszewski P (2014) Application of isotopic tracers as a tool for understanding hydrodynamic behaviour of the highly exploited Diass aquifer system (Senegal). *J Hydrol* 511:443–459
- Magee JW (2009) Palaeovalley groundwater resources in arid and semi-arid Australia: a literature review. *National Water Commission, Geoscience Record* 2009/03:224
- Meyer PS (2003) An explanation of the 1:500 000 general hydrogeological map. In: Bloemfontein 2924. *Geohydrology*, Department of Water Affairs & Forestry, Pretoria, Directorate
- Nanson GC, Croke JC (1992) A genetic classification of floodplains. *Geomorphology* 4:459–486
- Nowinski DJ, Cardenas MB, Lightbody AF (2011) Evolution of hydraulic conductivity in the floodplain of a meandering river due to hyporheic transport of fine materials. *Geophys Res Lett* 38:L01401
- Palmer MA (1993) Experimentation in the hyporheic zone: Challenges and prospectus. *J N Am Benthol Soc* 12:84–93
- Payne RR (1990) The use of stable isotope tracers for the estimation of the direction of groundwater flow. *J Hydrol* 112:395–401
- Ritter DF, Kinsey WF, Kauffman ME (1973) Overbank sedimentation in the Delaware River valley during the last 6,000 years. *Science* 179:374–375
- Shakhane T, Fourie FD, Du Preez PJ (2017) Mapping riparian vegetation and characterising its groundwater dependency at the Modder river government water scheme. *Groundw Sustain Dev* 5:216–228
- Sophocleous M (2002) Interactions between groundwater and surface water: the state of the science. *Hydrogeol J* 10:52–67
- Sophocleous M (2003) Environmental implications of intensive groundwater use with special regard to stream and wetlands. In: Llamas MR, Cursodio E (eds) *Intensives use of groundwater*. A.A. Balkema, Lisse, pp 93–112
- Uchida T, Asano Y, Onda Y, Miyata S (2005) Are headwaters just the sum of hillslopes? *Hydrol Process* 19:3251–3261
- Wen DG (2002) Application of the environmental isotopes to study on the attribution of regional groundwater resources. *Earth Sci* 27:141–147
- Winter TC (2001) The concept of hydrological landscapes. *J Am Water Resour Assoc* 37:335–349
- Winter TC, Harvey JW, Franke OL, Alley WM (1998) *Ground water and surface water: a single resource*, vol 1139. DIANE Publishing Inc., Darby, PA
- Wolman MG, Leopold LB (1957) River floodplains: some observations on their formation. *US Geol Surv Prof pap* 282C:87–107
- Wolock DM, Fan J, Lawrence GB (1997) Effects of basin size on low-flow stream chemistry and subsurface contact time in the Never-sink River watershed. *Hydrol Process* 11:1273–1286
- Woodford AC, Chevallier L (2002) *Hydrogeology of the Main Karoo Basin: Current knowledge and future research needs*. Water Research Commission report no. TT 179/02. Pretoria, South Africa